Journal of Thermal Analysis and Calorimetry, Vol. 65 (2001) 69–86

STRUCTURAL STUDIES ON PEK/TPI BLENDS

F. Cser[*] *and A. Goodwin*[**]

CRC for Polymers, 32 Business Dr., Notting Hill, VIC 3168 Australia and Department Materials Engineering, Monash University, Clayton, VIC 3168 Australia

(Received May 5, 2000; in revised form November 25, 2000)

Abstract

Blends of poly(ether ketone) (PEK) with poly(terephthaloyl-imide) (a thermoplastic polyimide, TPI) were studied by temperature-modulated DSC (TMDSC) and X-ray diffraction. Samples were prepared by compression moulding of the premixed materials at 400°C and quenched to prevent crystallisation.

The amorphous blends showed a single glass transition but with a jump in the temperature value at 60 mass% of PEK, indicating limited miscibility of the system at both sides of the composition series in the quenched, glassy state. Two cold crystallisation peaks over the concentration range 30 to 70 mass% of PEK were observed, but only one for all other compositions. A single melting peak was observed in all systems.

Blends crystallised from the glassy state showed eutectic behaviour with the presence of the crystals of both pure components. This is the first reported case of two semicrystalline polymers exhibiting eutectic co-crystallisation. The formation of eutectic crystals is proof of full miscibility of the two polymers in their liquid state, i.e. at a temperature of 400°C and above. Blends cooled from the melt at a cooling rate of 2 K min^{-1} showed a single glass transition and an extended melting range.

Crystallisation during a second melting run generally starts at a different temperature then during the first run indicating chemical changes occurred in the molten state. This change was also verified by an exothermic peak above the melting temperature using TMDSC.

Keywords: eutectic co-crystallisation, miscibility, poly(ether ketone), poly(terephthaloyl-imide)

Introduction

The poly(ether ketone) (PEK)/poly(terephthaloyl-imide) (TPI) two component blends were found by Sauer and Hsiao [1] to be an immiscible/semimiscible system in the solid state (there are two glass transitions on the TPI-rich side and only one glass transition at the PEK-rich side of the phase diagram, and their temperature values change continuously with the composition). The same system in the liquid state

* Author for correspondence. Recent address: Dept. Chemical and Metallurgical Engineering, RMIT University, P.O. Box: 2476V, Melbourne, VIC 3001, Australia

** Recent address: Boral Plasterboard, 676 Lorimer Str. Port Melbourne, VIC 3207, Australia

1418–2874/2001/ $ 5.00

Akadémiai Kiadó, Budapest

was described later by Sauer, Hsiao and Faron [2] to be either a fully miscible or an immiscible (two-phase) system with the upper critical mixing temperature of 440°C. This temperature depended on the mixing temperature. The blending of the components was carried out by Sauer and Hsiao without any mixing equipment at 415°C using a hot press at a very short time (1 min) [1].

These papers also proved the existence of a mixture with a lowest melting point, but the number of compositions was not sufficient to adequately interpret the data. The studies cited above [1, 2] were carried out by DSC using a 20 K min^{-1} heating rate. X-ray results were mentioned but primary data were not given in the papers.

Lu, Cebe and Capel [3] and Krüger and Zachmann [4] used small angle X-ray scattering (SAXS) and wide angle X-ray scattering (WAXS) to study crystallisation of TPI. TPI was aged at a temperature greater than 300°C and synchrotron radiation source was used in the SAXS studies. A single peak has been found in the Lorentz corrected SAXS intensities at s~0.005 ($Å^{-1}$). The use of Lorentz correction in this case is questionable as it may produce artificial peaks in the SAXS intensities [5, 6]. WAXS intensities showed two main peaks superimposed on an amorphous peak at 2Θ~19° and 23° (CuK_α). Huo, Friler and Cebe [7] used Avrami type analyses of cold crystallisation and attempted to determine the underlying physical nature of the cold crystallisation process.

As the system might have different phase relationships, the actual structure of the blend should be known before a detailed crystallisation kinetic study can commence. X-ray diffraction and temperature modulated DSC (TMDSC) were selected as investigating tools. This paper reports of the mentioned study.

Experimental

Methods

Sample preparation

Two series of samples were prepared using a Brabender twin screw extruder at a barrel temperature of 396°C. One set (PEK, TPI and blends of 25:75, 50:50 and 75:25) were compression moulded into films with a film thickness of 0.4–0.5 mm using a 390–396°C block temperature. The other samples (blends with composition of PEK:TPI 10:90, 30:70, 60:40 and 90:10 as well as new TPI) were compression moulded at 396–403°C block temperatures. The samples were placed in-between two Teflon sheets and placed in the press without pressure for 3–5 min (premelting). A pressure of ~5 kPa for an additional 2–3 min was then applied, the full process completed in 7–8 min. After the pressure was released the films and the teflon sheets were quenched in an ice-water bath. Transparent yellow-brownish films were obtained.

Crystallisation was achieved within the press at 325°C. The samples were annealed for 10 min at low pressure (<0.5 kPa). The well crystallised, fragile films were opaque. Two samples (25 and 50 mass% PEK) were annealed in a hot stage of an op-

tical microscope for 5–10 min. As the maximum temperature of the hot stage was 300°C, the cold crystallisation was not complete.

Sheets with a length of 22 and a width of 5 mm were cut from the films and a stack of 4–5 sheets were used for X-ray diffraction studies. Circular samples of 6 mm in diameter were cut with masses between 8 and 15 mg and used for the TMDSC studies. TPI and the blends of 25:75, 50:50 and 75:25 were tested twice by TMDSC using samples cut from different positions of the film.

X-ray diffraction

A Rigaku Geigerflex generator was used with a wide angle and a Kratki type small angle goniometer. An accelerating voltage of 30 kV and 30 mA current was applied using Ni filtered CuK_{α} radiation. Intensity data were recorded on a floppy disk and the data processing was carried out separately using software written by one of the authors.

WAXS

WAXS intensities were collected from $2\Theta=3$ to 50° by transmission techniques on compression moulded samples using a film stack with an overall material thickness of 1.5–2 mm. A scanning rate of $2\Theta=2°$ min^{-1} was used and $\Delta 2\Theta=0.04°$ steps applied.

SAXS

SAXS intensities were collected from $2\Theta= -1$ either to 1° or to 3° in steps of 0.002 degrees using the same samples as used for WAX in transmission mode. The scanning rates were $\Delta 2\Theta=0.04$ or 0.08° min^{-1}. Background intensities were collected from each sample positioned just in front of the counter. Primary data were processed by removing the background and calculating the average of the two sides of the diffraction data using SAXS computer program developed by one of the authors.

The maximal resolution of the SAXS camera was 120 nm as the intensities could be collected generally at diffraction angle, $2\Theta \geq 0.06°$. As the SAXS intensities showed no peak characteristic of a reciprocal lattice, i.e. they showed a particle scattering only, no Lorentz correction was applied [6]. SAXS data are represented in both Guinier ($\ln(I)$ *vs.* s^2) and in fractal ($\ln(I)$ *vs.* $\ln(s)$) plots, where $s=4\pi\sin(\Theta)/\lambda$.

Thermal analysis

The blends and their components were tested by a TA Instruments TMDSC of type 2920 equipped with LNC unit. The melting, the crystallisation and the glass transitions of the blends were analysed and their parameters represented as a function of the composition.

Two cycles of TMDSC test were performed on each sample. 2 K min^{-1} underlying heating and cooling rates were applied using ±0.6 K modulation amplitude and p=40 s modulation period with He as purge gas with a 90 ml min^{-1} flow rate. A medium value of the modulation period was used because of the possible high rate of crystallisation. A me-

dium amplitude was also used (slight cooling on heating [8]) to have a better chance of obtaining a comprehensive value of the glass transition temperature.

The first cycle started at 70 and was completed at 400°C. Then the sample was cooled to 70°C. In the second cycle, the sample was heated again to 400°C followed by cooling to room temperature. According to our previous experience for most semicrystalline polymers, the second cooling cycle results in the same DSC curve as the first one, but samples reported in this work, exhibited different behaviour.

Results

WAXS

Figure 1 show the WAXS intensities of the quenched samples. The WAXS curve indicates completely amorphous materials. The peak position of both basic materials are the same (2Θ=19°). Nevertheless, TPI has a broader diffraction peak than PEK. Furthermore, TPI has an additional small peak at 2Θ=5°, which corresponds to a Bragg period of 1.8 nm. The blends with TPI content of more than 40% also show this peak, and the peak maximum intensity increases with increasing TPI content.

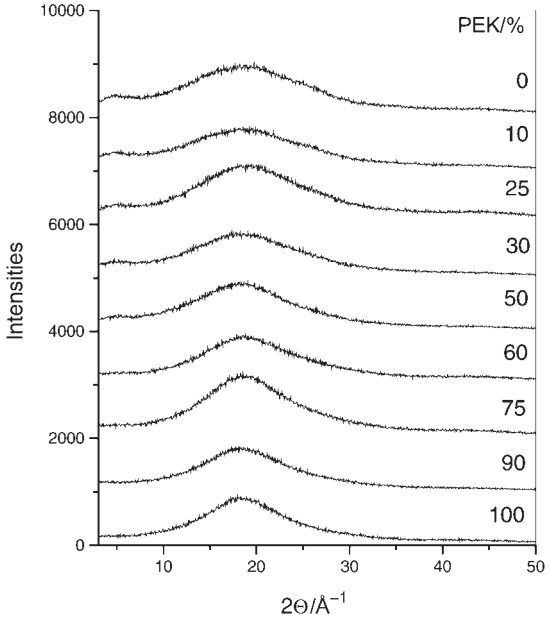

Fig. 1 WAXS intensities of quenched samples of TPI/PEK blends

Figure 2 represents the WAXS intensities of the annealed materials. TPI has an intensive peak at 2Θ=3.5° (a Bragg period of 2.5 nm), and this peak is useful for the detection of crystalline TPI in the blends. There are small differences in the intensi-

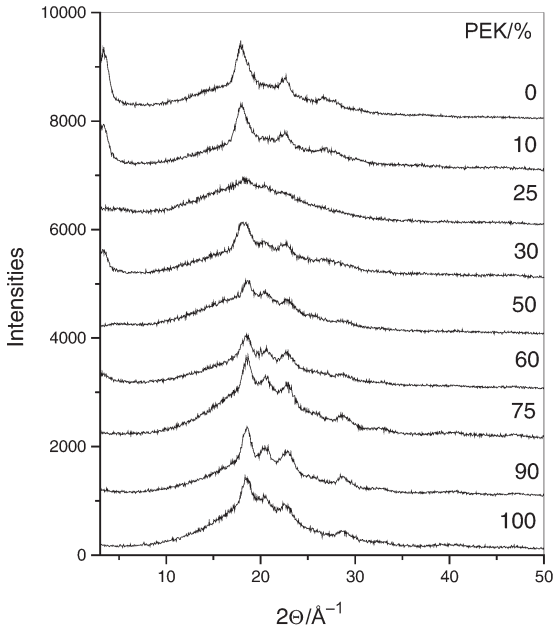

Fig. 2 WAXS intensities of annealed samples of TPI/PEK blends

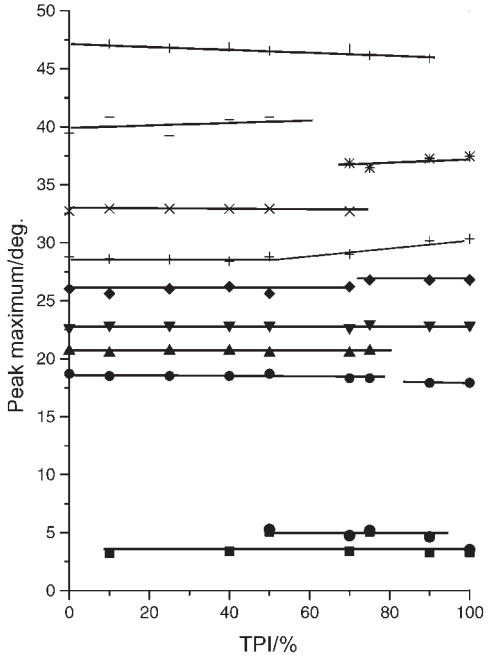

Fig. 3 WAXS crystalline peaks as the function of the composition for PEK/TPI blends

ties of the main diffraction peaks (2Θ=16–25°) of the two materials. PEK has an additional peak at 2Θ=20° which can be used for the detection of the presence of crystalline PEK in a blend. Two blends (with a PEK content of 25 and 50%, respectively) were not fully crystallised. They do not exhibit the peak characteristics of crystalline TPI, but rather show the broad peak characteristics of amorphous TPI.

Figure 3 displays the Bragg peak positions as a function of composition. Parallel lines can be seen starting from each of the pure components, but the lines move only to parallel or something like that. One peak has a non-constant value, increasing with increasing TPI content above 50% of TPI content.

The peak characteristic for TPI can be found in all of the blends, including that with a 40% TPI content. The peak characteristics of PEK are present in the blends up to 30% PEK. The peak maxima are independent of the composition, while the intensities of the peaks decrease proportionally with the decrease of the component associated with the peak. This behaviour can be found in eutectic crystallisation of two independent crystalline materials. The thermodynamic condition to form eutectic crystals is the mutual miscibility of the components in the liquid state of melt.

SAXS

The SAXS intensities of the amorphous samples are shown in Fig. 4. At diffraction angles higher than 0.5° the SAXS intensities are small i.e. they are lost in the noise. They best fit a straight line in the lg(I) *vs.* log(s^2) representation (where $s=4\pi\sin(\Theta)/\lambda$) following a fractal type of scattering. There are no meaningful differences in the scattering intensities between the basic components and the blends. This means that these amorphous materials have a fractal type structure. This might be an indication of miscibility of the two components at a non-molecular level (like colloids).

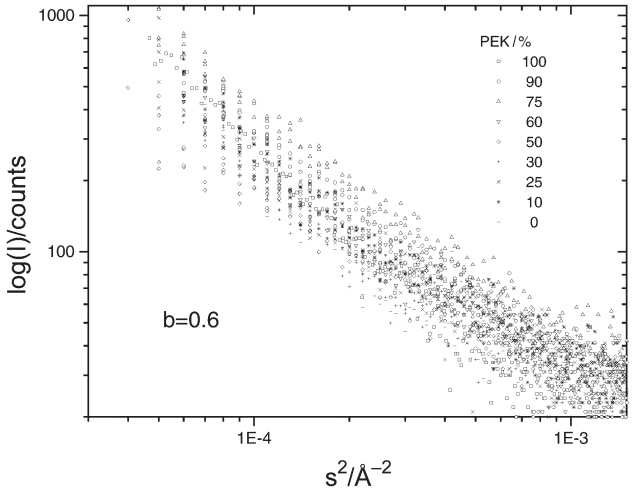

Fig. 4 SAXS intensities of quenched samples of blends of PEK and TPI

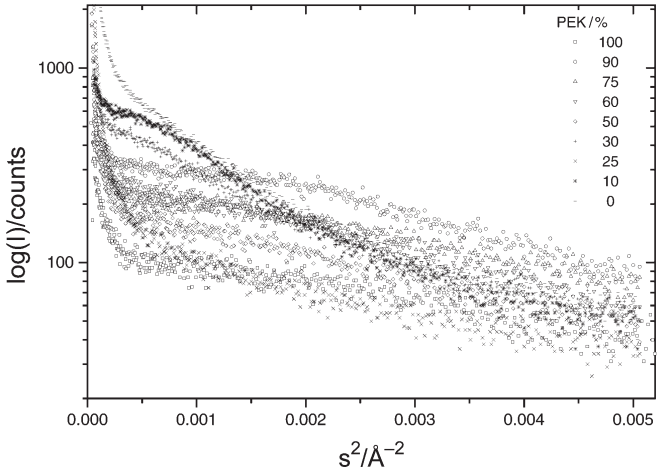

Fig. 5 SAXS intensities of annealed samples of the blends of PEK and TPI

SAXS intensities of the annealed samples are shown in Fig. 5 as a Guinier representation. Crystalline samples did not show a well defined peak in their SAXS curves with the exception of TPI, for which the SAXS intensities show a broad maximum at 2Θ=0.34° (i.e. 26 nm). PEK and some of the blends also have a very broad maximum at 2Θ~0.4°. The intensities are two orders of magnitude higher for crystalline samples than for the amorphous materials at diffraction angles over 0.5°.

TMDSC

Figure 6 shows the TMDSC curves of the total heat flow, and Fig. 7 represents the corresponding kinetic heat flows as the function of temperature for the basic materials recorded in the first heating cycles.

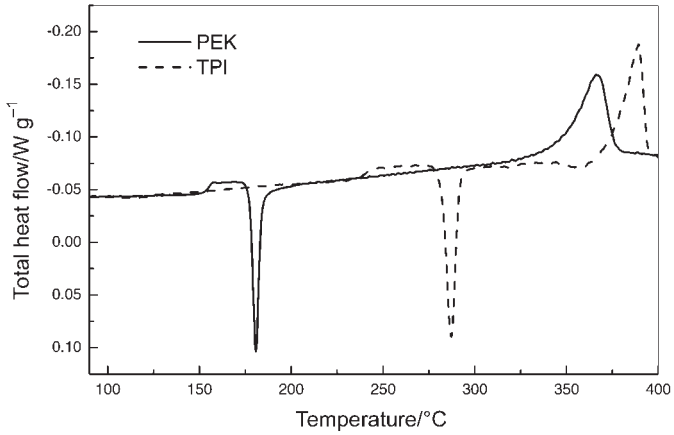

Fig. 6 TMDSC total heat flow curves of PEK and TPI recorded in the first heating cycles, respectively

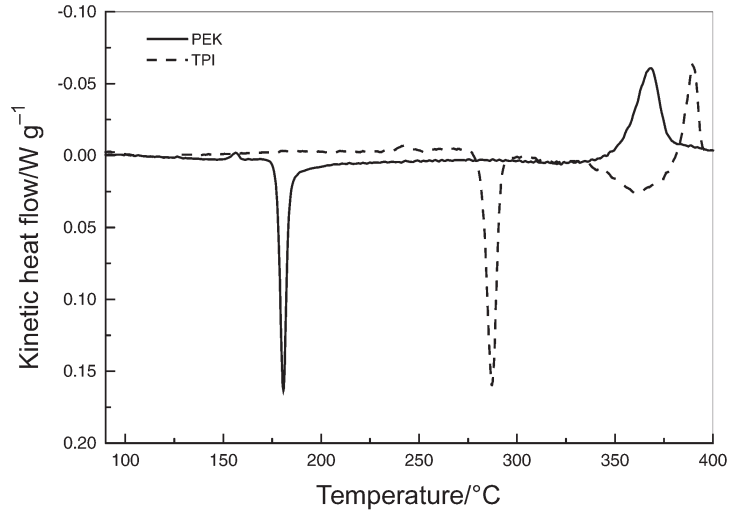

Fig. 7 TMDSC non-reversing heat flow curves of the basic components recorded in the first heating cycles respectively

The first transition is a step into the exothermic direction representing the glass transition (at 158°C for PEK and 240°C for TPI). This step is absent in the kinetic heat flow curves but there is a small exothermic relaxation peak as a consequence of the quenching. The glass transition is followed by an exothermic peak indicating cold crystallisation. After the cold crystallisation peak crystallisation continues up to the beginning of the melting, as seen in the kinetic heat flow curves (Fig. 7). TPI has a stronger secondary crystallisation before the melting endotherm as indicated by a

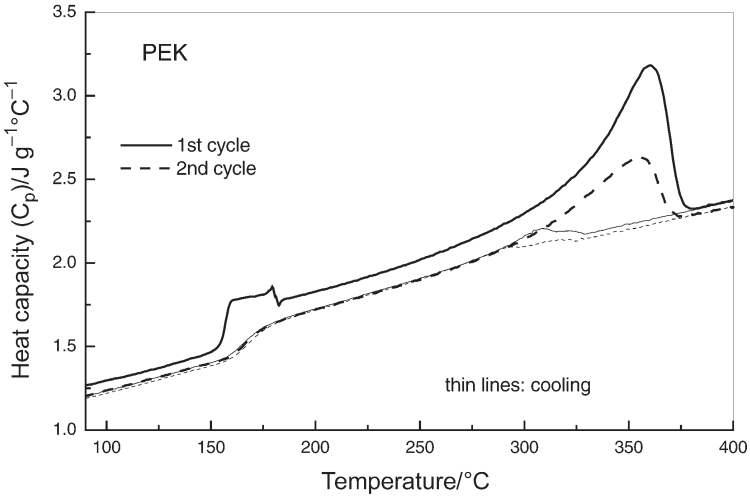

Fig. 8 TMDSC heat capacity curves of PEK recorded in two consecutive heating and cooling cycles

broad exothermic peak in the kinetic heat flow curve. This exothermic peak is also visible in the total heat flow curve just below the melting peak.

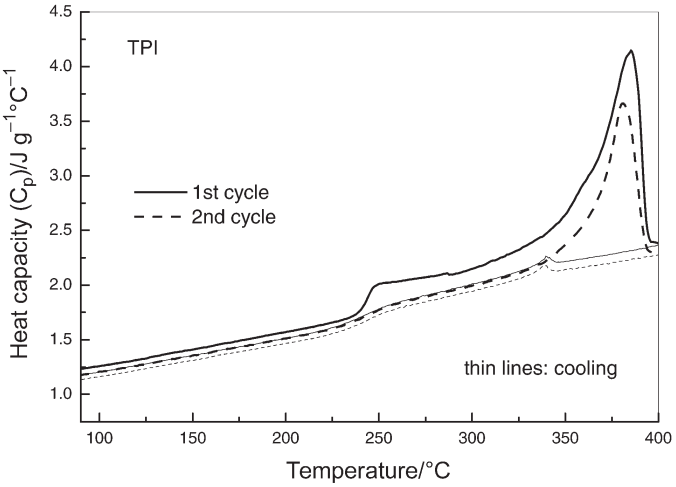

Fig. 9 TMDSC heat capacity curves of TPI recorded in two consecutive heating and cooling cycles

Figures 8 and 9 represent the heat capacity curves of the two basic materials recorded in two consecutive heating and cooling cycles. As expected, the glass transition is visible as endothermic steps. The cold crystallisation process is absent in the curves. Nevertheless there is a sudden decrease in the heat capacities corresponding to those of the semicrystalline system. The endothermic step indicating the end of the cold crystallisation process is smaller in TPI than in PEK.

The first cooling cycle and the second heating cycle show the same heat capacity function below the crystallisation temperatures for both materials. This temperature is used as the lower limit of integration for the determination of the transition enthalpies. The heat capacities of the second cooling cycle are the same as those during the first one for PEK. However, c_p (second cycle)<c_p (first cycle) for TPI. This is an indication of some irreversible change of the polymer in the molten state, above its melting temperature. The glass transition temperature of the semicrystalline systems is higher than that of the totally amorphous samples as for many semicrystalline polymers. There is no major shift in the glass transition temperature in the cooling cycles with respect to the second heating run.

The total heat flow curves of the first heating cycle of the basic materials and those of the blends are compared in Fig. 10. There are two cold crystallisation peaks in the blends with 60 and 50% of PEK content. The blends with lower and higher PEK content show only one cold crystallisation peak. There is double melting peak in blends with PEK content of 60 and 30%. A shoulder at the lower temperature side of the melting peak can also be seen in blends with PEK contents of 25 and 10%.

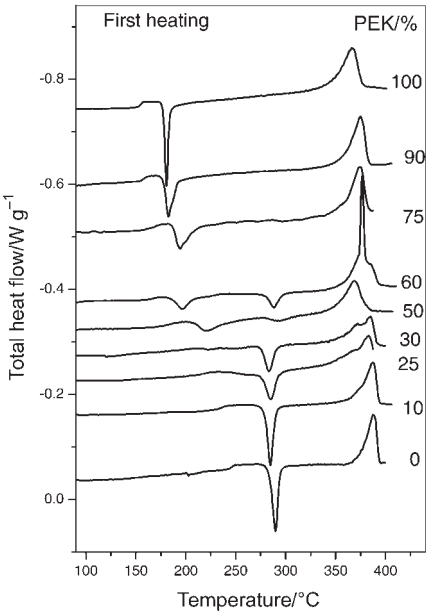

Fig. 10 TMDSC total heat flow curves of the blends of PEK with TPI recorded in the first heating cycle. Figures on the curves indicate the PEK content of the sample

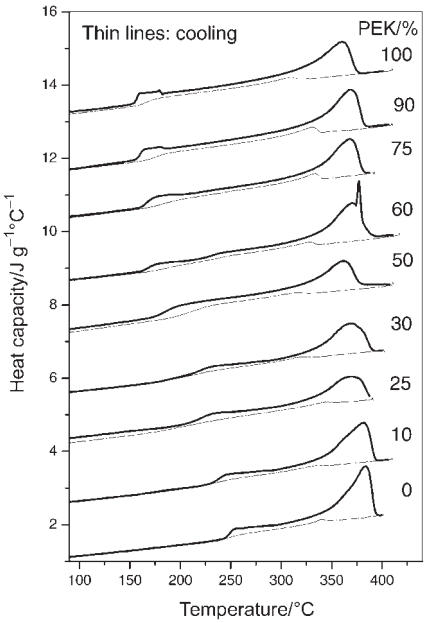

Fig. 11 TMDSC heat capacities flows of the blends of PEK with TPI recorded in the first heating and cooling cycles. Figures on the curves indicate the PEK content of the sample

The heat capacities of the same materials recorded in the first heating and cooling cycles are shown in Fig. 11. There is only one step characteristic of the glass transition temperature of the blends and their location along the temperature scale is not a constant. The melting peaks (corresponding to reversing melting) show mainly a single peak, but a sharp peak can also be seen in the blend with 60% of PEK. This sample showed also two glass transition temperatures and its melting peak is very sharp, with a shoulder at the upper temperatures indicating a maximal temperature of an annealing (mixing?) of ~370°C. There are two other samples with small shoulders on their melting peak (25 and 10% PEK).

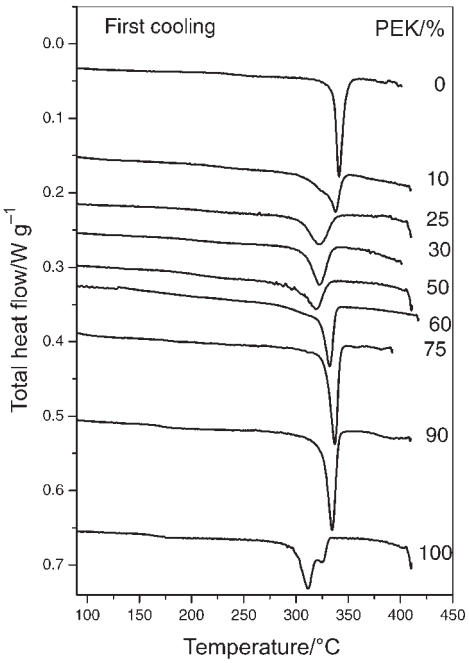

Fig. 12 TMDSC total heat flows of the blends of PEK with TPI recorded in the first cooling cycle. Figures on the curves indicate the PEK content of the sample

The total heat flow curves of the first cooling cycle are compared in Fig. 12. The crystallisation during the first heating cycle resulted in a single crystallisation peak with the exception of TPI, where a double peak is seen. The peak temperature of the crystallisation has a minimal value at 50% PEK content.

The glass transition temperature (maximal slope), the onset and the peak of cold crystallisation recorded in the first heating cycle are shown in Fig. 13 as a function of the composition. Both transitions have a break at 30% PEK content. Each part of the diagram indicate miscibility of the two materials. The complete diagram can be interpreted as a single phase system with limited miscibility at both sides. The glass transition temperature shows greater concentration dependence at the TPI side of the dia-

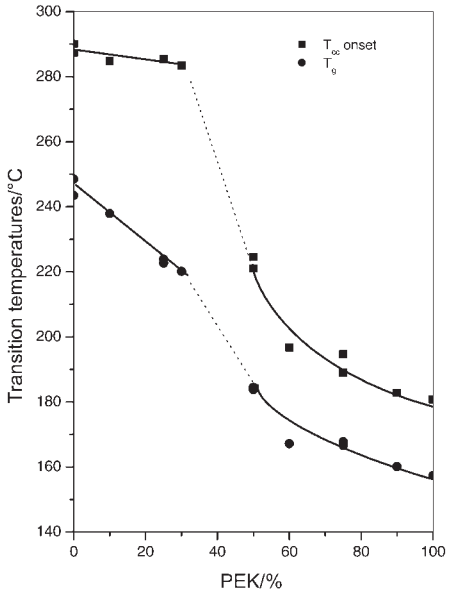

Fig. 13 Glass transition temperature (T_g), and starting temperatures of the cold crystallisation (T_{cc} onset) of quenched samples of the blends of PEK with TPI as the function of the composition

gram, the PEK side being nearly constant. There is a jump between the two structures at 25–40% PEK content.

The first heating cycle shows the thermal history of the systems as a result of quenching of the liquid formed at or above 400°C. The second heating and cooling cycles show the system formed under a slow cooling conditions (2 K min^{-1}), and these are somewhat closer to the equilibrium conditions. Naturally, full equilibrium cannot be achieved at any rates of cooling.

The total heat flows recorded in the second heating cycle are compared in Fig. 14. The heat capacities recorded in the second heating and cooling cycles are shown in Fig. 15, and the total heat flow curves recorded in the second cooling cycle are compared in Fig. 16.

There is generally one melting peak in the heating cycles of the blends. Blends with 30 and 25% of PEK content show double peaks in the total heat flow curves. This is not seen in the heat capacity curves as only the blend with a 25% of PEK content shows a shoulder in its melting peak. There is only one-step characteristic of the glass transition and T_g changes with composition, decreasing with increasing PEK content of the blends. T_g changes linearly with composition (Fig. 17). The starting temperature of the endotherm peak recorded in the first heating cycle varied with the composition, but those recorded in the second heating cycle seem to be constant. The peak melting temperatures show a minimum at 50 and a maximum at 75% of PEK content. The TPI side of the diagram shows an increasing melting peak temperature

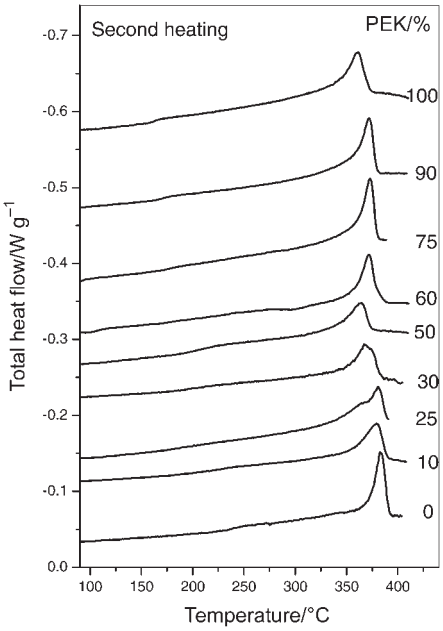

Fig. 14 TMDSC total heat flows of the blends of PEK with TPI recorded in the second heating cycle. Figures on the curves indicate the PEK content of the sample

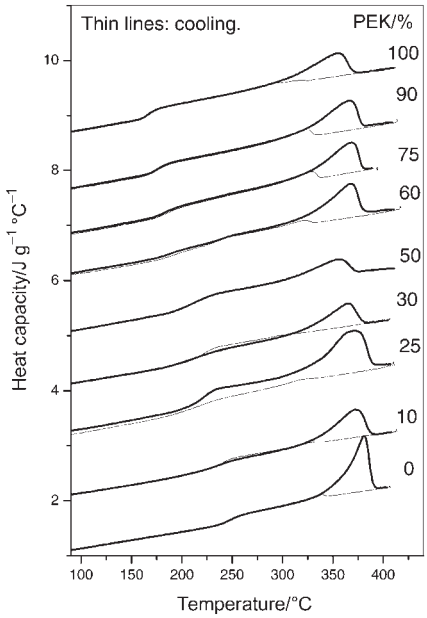

Fig. 15 TMDSC heat capacities of the blends of PEK with TPI recorded in the second heating and cooling cycles. Figures on the curves indicate the PEK content of the sample

with increasing TPI content after the minimum. The crystallisation temperatures show a definite double character and a minimum at 40–50% of PEK content.

The crystallisation temperatures show definite changes with respect to the first cooling cycles (compare Figs 12 and 16). Exothermic heat flows are visible upon cooling in most of the samples in their liquid state before the crystallisation commences (see declining curves in Figs 12 and 16). This is a further indication of chemical reaction in temperatures when the material was in the melt.

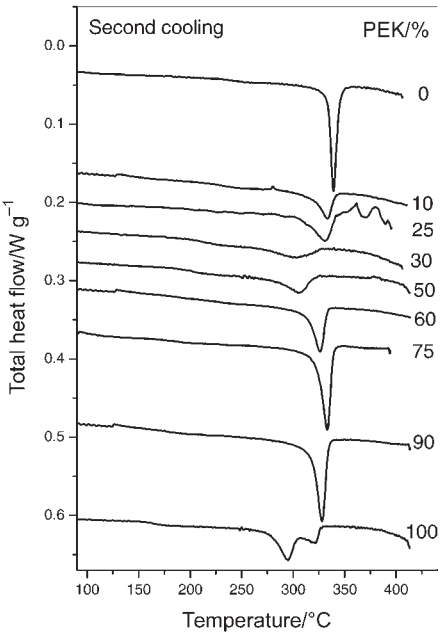

Fig. 16 TMDSC total heat flow curves of the blends of PEK with TPI recorded in the second cooling cycle. Figures on the curves indicate the PEK content of the sample

The heats of transitions integrated from the total heat flow curves are shown in Fig. 18 as a function of the composition. The heat of fusion shows a linear composition dependence in the first heating cycle but eutectic like dependence for the second heating cycle. This suggest, there may be a linear decreasing heat of fusion with increasing concentration of the second component, leading to the minimum taking place between 30 and 50% PEK content. The heat of cold crystallisation has a minimum at the same composition, but the heat of crystallisation recorded in the two cooling cycles exhibits a minimum at 30–50 and a maximum at 75–90% PEK content.

The temperature of cold crystallisation depends on the composition (Fig. 13 peak temperature (T_{cc} onset)). There are two distinct temperature ranges where the cold crystallisation takes place. Samples with TPI content of less than 50% show a lower peak temperature (180–190°C) of cold crystallisation than samples with TPI content above 50% (270–280°C). The melting temperatures and the crystallisation

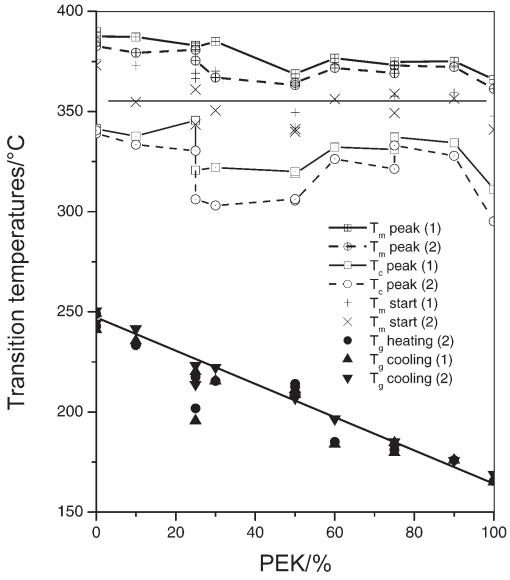

Fig. 17 Glass transition temperatures, starting and peak temperatures of the melting and of the crystallisation as a function of the PEK content of the blends obtained from TMDSC total heat flow curves in the first and in the second heating and cooling cycles respectively

temperature from the melt show some correlation. They increase with respect to those of PEK with a minimum at 50% TPI content. Then they rise again up to those of the pure TPI. However, the scatter of the data is large.

The reproducibility of the melting curves is good. The DSC-curves of the second cooling cycles differ greatly from those of the first, to a degree much greater than the experimental error. The DSC-curves of the second TPI sample showed greater differences from those of the first TPI samples (not shown in the figures).

The heat capacity charts also show great changes during these cycles. There is only one glass transition temperature of the completely amorphous materials, with the exception of sample with 40% TPI content. The glass transition temperatures in both cooling cycles and in the second heating cycle (Fig. 17) show a nearly linear dependence on composition, both for the amorphous and the crystallised materials. The crystallised samples show generally higher glass transition temperatures than the amorphous ones, the difference of these two being greatest in the middle of the composition range. The scattering of data is considerable. The glass transition temperature of the second cycle at the PEK-rich blends is higher than that of the first cycle, for TPI-rich blends this is not the case. The lower glass transition temperature of the anomalous blend with 60% of PEK content increases with longer heat treatment, the intensity (height of the step) of the upper component simultaneously decreasing. This indicates a continuous dissolving of TPI in the PEK matrix (much below the upper critical mixing temperature given by [2]).

The heat capacity values on cooling in the second cycle are smaller than those in the first cycle. This phenomenon (together with the exothermic heat found on the kinetic heat flow charts above the melting temperatures) is an indication of some chemical reaction within the blend in the state of melt.

The non-reversing recordings gave very noisy DSC curves above the melting temperature and during the crystallisation recorded subsequent on cooling. This type of noise is not normally observed by the same equipment on semicrystalline polymers. The exothermic heat flow above the melting temperature is the same as in the total heat flow curves. These charts (not shown in this paper but available upon request) also show additional crystallisation following the cold crystallisation peak in the first heating cycle. There is an endothermic change of slope in the total heat flow curves in the second heating cycle starting at ~200–220°C (Fig. 14) what is not present in the heat capacity curves (Fig. 15), indicating the true onset of the melting at these temperatures, i.e. the solution of the polymeric crystals in another phase. This kind of behaviour is typical for eutectics where the excess crystals are dissolved in the molten eutectics. There is no peak in the DSC curves, which would show the melting of the eutectic itself.

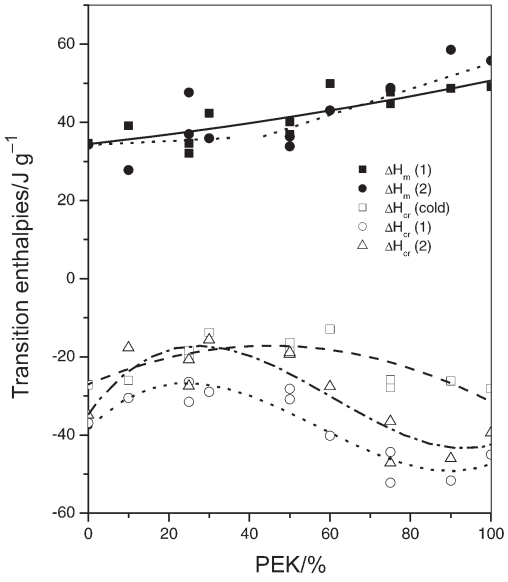

Fig. 18 Enthalpies of the fusion ($\Delta H_m(1)$, $\Delta H_m(2)$) and crystallisation (ΔH_{cr} (1), ΔH_{cr} (2), ΔH_{cr}(cold)) integrated from the total heat flow curves of blends of PEK with TPI as the function of the composition. 1 and 2 refer to first or second cycle, cold refers to cold crystallisation

The heat of fusion and the heat of the crystallisation from the melt obtained from the total heat flow curves show a maximum at 25–50% PEK content (Fig. 18). The data are scattered and therefore only trends can be deduced.

Discussion

TPI forms crystals where the longest Bragg period (2.5 nm) corresponds to the length of the monomeric units in an extended chain conformation of the macromolecule. In the melt the Bragg period (1.8 nm) indicates a 45° decline within the chains (SQRT(2)/2). Therefore the 4–6 nm lamellar thickness of the TPI crystals given in reference [3] (Fig. 8b) seems not to be realistic.

The PEK/TPI systems seem to form a fully miscible series in the melt which is retained in the quenched, glassy phase on a macroscopic (super-molecular) scale. In order to achieve full miscibility, the system needs a mixing temperature above the melting point of the TPI (i.e.>390°C) and some time to allow for the completion of the mixing. SAXS intensities show much more fractal-type two-phase systems than full miscibility on molecular level. There are traces of both crystalline materials in the cold crystallised systems detected by WAXS, but their presence cannot be seen on the DSC curves (there are no double melting peaks in most of the DSC curves). The resolution of TMDSC should make it possible to resolve the double peaks, even in the case of materials with melting point as close the ones as studied here. A eutectic type phase structure is characteristic of such a crystallised system. As far as we know polymeric systems with such a eutectic type of interaction have not been previously described in the literature.

The instability of the systems is remarkable. The reproducibility of the DSC curves of samples cut out from the same sheet from different positions is very poor. The second cooling cycle is different than the first one and there is a great change in the heat capacity values between the first and the second cycles (e.g. the whole temperature range for the blend of 50% PEK content). The change in the properties takes place above the melting temperatures as there is exothermic process, and the heat capacities decrease in this period of the cycles. The heat capacities in the second heating cycle are practically the same as those in the first cooling run up to the melting range. The decrease in the heat capacity values in the second cooling cycle with respect to the first one happens when the material is heated above its melting range. The calorimetric data (heats of transitions) do not form a smooth function of composition, and their scatter is considerable.

Conclusions

The PEK and TPI form fully miscible blends above the melting temperature of the TPI and it is not necessary to heat the system above 440°C to achieve this miscibility. They form eutectic systems by cold crystallisation when the amorphous material is heated above the glass transition temperature. The melting point of the eutectic mixture is estimated to be 200–230°C. When the glass transition temperature of the system is higher than this value, the crystallisation of the eutectic on cooling or on heating is restricted (TMDSC, 2 K min^{-1}). Only crystals of the excess components are formed.

The system is not suitable for carrying out reproducible, comprehensive crystallisation kinetic studies due to the thermodynamical instability of the materials. A method of reproducible production of amorphous samples should be determined. The data obtained in this study are not consistent with previous literature data.

* * *

The authors are indebted to Dr. M. Zipper for his participation in the experimental work and for Dr. G. P. Simon for useful discussions.

References

1 B. B. Sauer and B.S. Hsiao, Polymer, 34 (1993) 3315.
2 B. B. Sauer, B. S. Hsiao and K. L. Faron, Polymer, 37 (1996) 445.
3 S. X. Lu, P. Cebe and M. Capel, J. Appl. Polymer Sci., 57 (1995) 1359.
4 K. N. Krüger and H. G. Zachmann, Macromolecules, 26 (1993) 5202.
5 J. Dlugosz, G. V. Fraser, D. Grubb, A. Keller, J. A. Odell and L. Goggin: Polymer, B17 (1976) 471.
6 F. Cser, J. Appl. Polym. Sci., 80 (2001) 358.
7 P. P. Huo, J. B. Friler and P. Cebe, Polymer, 34 (1993) 4387.
8 F. Cser, F. Rasoul and E. Kosior, J. Thermal Anal., 50 (1997) 727.